An Optical Frequency Shifter Based on High-Order Optical Single-Sideband Modulation and Polarization Multiplexing

Xuan Li, Shanghong Zhao, Zihang Zhu, Kun Qu, Tao Lin, and Shilong Pan, *Senior Member, IEEE*

Abstract—We propose and experimentally demonstrate a novel electro-optic frequency shifter with frequency multiplication operation based on high-order optical single-sideband (SSB) modulation and polarization multiplexing using an integrated dual-polarization quadrature phase shift keying (DP-QPSK) modulator. By changing the dc bias phases of the modulator and the phase difference between the input RF signals, two-high-order SSB modulation signals are generated from the two QPSK modulators. After that, the two optical signals are polarization multiplexed and then projected to one direction to remove the low-order sidebands while only the high-order sideband is reserved. The scheme is numerically analyzed with the modulation indices of the modulator for optimal operation. A distinct advantage of this approach is the capability to generate a frequency shifting with a continuous and ultrawide tunable range (more than ± 100 GHz), and the tuning operation is accurate, simple, and flexible. An experiment is carried out to achieve a frequency-doubled optical frequency shifter. A continuous frequency shifting ranged from -36 to 36 GHz is experimentally verified.

Index Terms—Microwave photonics, optical frequency shifter, polarization multiplexing, single-sideband modulation.

I. INTRODUCTION

O PTICAL frequency shifter is a key technique in heterodyne interfering and optical frequency synthesizing, and has wide applications in scientific measurement, high-speed optical communication, optical sensors and lidar systems [1]–[8].

Various methods have been proposed and demonstrated to realize an optical frequency shifter. Generally, an optical frequency shifter can be achieved based on acousto-optic or thermo-optic effects with compact integration [9]–[11]. The main drawback of these methods is that only a small frequency shifting can be obtained due to the limited bandwidth of the acousto-optic or thermo-optic modulators (below a few GHz). Another widely investigated method to realize an optical frequency shifter is based on electro-optic effect [12]–[18]. For example, an optical frequency shifter can be achieved by using the slant periodic-domain inversion of a Bragg-type electro-optic traveling-phase grating (ETPG) [12]. This approach can provide wide tunable range for the frequency shifting of the generated signal (from few GHz to several tens of GHz). However, the frequency shifting is determined by the angle between the device and the input light, which makes the controlling and tuning operation complicated and difficult. To obtain a flexible and accurate frequency shifting, the optical single-sideband carrier-suppressed (SSB-CS) modulation technique is proposed [13]–[17], which can be realized by employing an Sagnac loop incorporating an electro-optic modulator [13], [14], a single-electrode Mach-Zehnder modulator (MZM) followed by an optical filter [15], a dual-electrode MZM followed by a polarizing element [16], or a simple quadrature phase shift keying (QPSK) modulator [17]. However, the previous SSB-CS modulation schemes can only generate a lower or upper first-order sideband, which makes the frequency shifting and its tunable range still limited by the bandwidth of the modulator and microwave devices (usually below 40 GHz). To overcome this problem, frequency multiplication is highly desired when performing the optical frequency shifting. Previously, a frequency-doubled optical frequency shifter was reported by using cascaded ETPGs [18], in which the frequency shifting of the generated optical signal was increased to 32.5 GHz with a 16.25 GHz RF signal. Similarly, the key disadvantage of this approach is the difficulty of the tuning operation.

In this paper, we propose a novel electro-optic frequency shifter with frequency multiplication operation based on optical high-order single-sideband (SSB) modulation and polarization multiplexing. The key component of the shifter is an integrated dual-polarization QPSK (DP-QPSK) modulator, which consists of a 3-dB optical coupler, two QPSK modulators and a polarization beam combiner (PBC). Compared with the previously proposed schemes, the new optical frequency shifter has a changeable multiplication factor of 2 or 3, which can achieve a frequency shifting beyond the operation bandwidth of the modulator and microwave devices. At the same time, the proposed shifter can provide a continuous and ultra-wide tunable range for the generated frequency shifting as no optical or electrical filter is involved, and the tuning operation is accurate, simple and flexible.

X. Li is with the School of Information and Navigation, Air Force Engineering University, Xi'an 710077, China, and also with the Key Laboratory of Radar Imaging and Microwave Photonics, Ministry of Education, Nanjing University of Aeronautics and Astronautics, Nanjing 210016, China (e-mail: lixuanrch@163.com).

S. Zhao, Z. Zhu, K. Qu, and T. Lin are with the School of Information and Navigation, Air Force Engineering University, Xi'an 710077, China (e-mail: zhaoshangh@aliyun.com; zhuzihang6@126.com; m13259463680@163.com; ltzhineng@163.com).

S. Pan is with the Key Laboratory of Radar Imaging and Microwave Photonics, Ministry of Education, Nanjing University of Aeronautics and Astronautics, Nanjing 210016, China (e-mail: pans@nuaa.edu.cn).

Color versions of one or more of the figures in this paper are available online at http://ieeexplore.ieee.org.
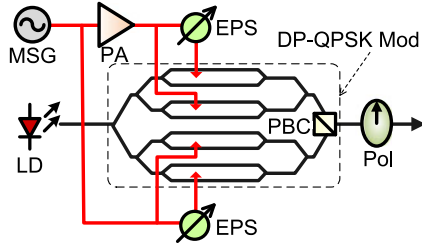
Digital Object Identifier 10.1109/JLT.2016.2611018

Fig. 1.   Schematic configuration of the proposed optical frequency shifter with frequency multiplication operation (LD: laserdiode; MSG: microwave signal generator; PA: power amplifier; EPS: electrical phase shifter; PBC: polarization beam combiner; DP-QPSK Mod: dual-polarization quadrature phase shift keying modulator; Pol: polarizer.

The remainder of this paper is organized as follows. In Section II, the principle of this novel proposed optical shifter is analyzed with theoretical and numerical investigation. Section III presents the experimental setup and results. Finally, the work is summarized in Section IV.

II. Principle and Theoretical Investigation

Fig. 1 shows the schematic configuration of the proposed optical frequency shifter with frequency multiplication operation, which consists of a laserdiode (LD), an integrated DP-QPSK modulator and a polarizer (Pol). The linear polarized light wave from the LD can be expressed as $E_{in}e^{j\omega_0 t}$, where E_{in} and ω_0 are the amplitude and angular frequency of the light, respectively. The light wave is sent to the DP-QPSK modulator, which consists of a 3-dB optical coupler, two QPSK modulators and a PBC, as shown in the figure. For actual implementation and simple analysis, the two QPSK modulators are identical and each of them consists of two identical sub-MZMs placed parallel in a main-MZM. For a single sub-MZM of the upper QPSK modulator driven by an RF signal, the modulated optical signal can be expressed by the Jacobi-Anger expansion as

$$
\begin{aligned}
E_m(t) &= \frac{1}{4}E_{in}e^{j\omega_0 t}\left\{ e^{j\left[m_1\cos(\omega t+\varphi)+\frac{\theta_0}{2}\right]} \right. \\
&\quad \left. + e^{j\left[-m_1\cos(\omega t+\varphi)-\frac{\theta_0}{2}\right]} \right\} \\
&= \frac{1}{4}E_{in}e^{j\omega_0 t}\left\{ \begin{array}{l} \sum_{n=-\infty}^{\infty} e^{j\frac{\theta_0}{2}}J_n(m_1)e^{jn\left(\omega t+\varphi+\frac{\pi}{2}\right)} \\ +\sum_{n=-\infty}^{\infty} e^{-j\frac{\theta_0}{2}}J_n(m_1)e^{jn\left(\omega t+\varphi+\frac{3\pi}{2}\right)} \end{array} \right\} \\
&= -\frac{1}{2}E_{in}e^{j\omega_0 t}\sum_{n=-\infty}^{\infty}\cos\left(\frac{\theta_0}{2}-\frac{n\pi}{2}\right)J_n(m_1)e^{jn(\omega t+\varphi)}
\end{aligned}
\tag{1}
$$

Here the insertion loss of the modulator is neglected, $m_1 = \pi V/(2V_\pi)$ is the modulation index, V is the amplitude of the RF signal, V_π is the half-voltage of the sub-MZM, ω and φ are the angular frequency and initial phase of the RF signal, respectively, θ_0 is the DC bias phase of the sub-MZM, J_n is the nth-order Bessel function of the first kind.

An electrical phase shifter (EPS) is employed to introduce a phase difference of $\Delta\varphi$ between the two RF signals applied to the two sub-MZMs of the upper QPSK modulator. The two
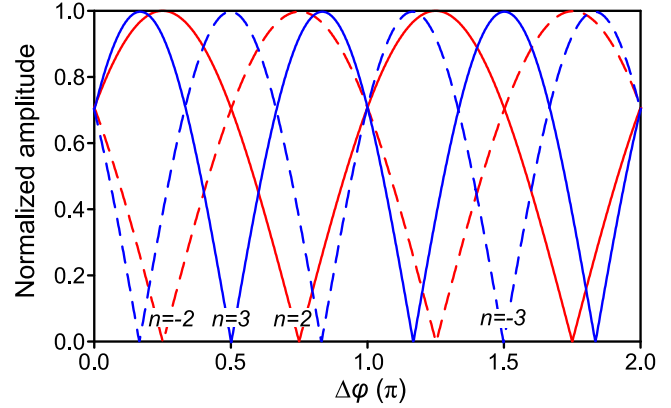

Fig. 2.   The calculated amplitude of second- and third-order sidebands varying with the phase difference.

sub-MZMs have same DC bias phase of θ_0 and the main-MZM has a DC bias phase of θ_m. Then the optical signal at the output of the upper QPSK modulator is given by

$$
\begin{aligned}
E_{up}(t) &= -\frac{\sqrt{2}}{4}E_{in}e^{j\omega_0 t}\sum_{n=-\infty}^{\infty}\cos\left(\frac{\theta_0}{2}-\frac{n\pi}{2}\right)J_n(m_1) \\
&\quad \times \left[\begin{array}{l} e^{j\frac{\theta_m}{2}}e^{jn(\omega t+\varphi)} \\ +e^{-j\frac{\theta_m}{2}}e^{jn(\omega t+\varphi+\Delta\varphi)} \end{array}\right]
\end{aligned}
\tag{2}
$$

To achieve the high-order SSB modulation, the nth-order sideband should be generated with the $-n$th-order sideband be suppressed. Fig. 2 shows the calculated amplitude of second- and third-order sidebands varying with the phase difference $\Delta\varphi$ when the DC bias phase θ_m is $\pi/2$. It can be seen that, the amplitudes of the sidebands are changed periodically and the $\pm n$th-order sidebands have opposite trend along with the variation of the phase difference, one of them can be totally suppressed while the other keeps the maximum by setting a proper phase difference $\Delta\varphi$. As a result, the high-order SSB modulation can be realized by using a QPSK modulator.

To achieve the Nth-order SSB modulation, the following condition should be satisfied

$$
\begin{aligned}
N\Delta\varphi+\theta_m &= (2k+1)\pi \\
N\Delta\varphi-\theta_m &= 2k\pi
\end{aligned}
\tag{3}
$$

Where k is an integer. The condition can be satisfied by setting the parameters as

$$
\theta_m = \frac{\pi}{2},\ \varphi = 0,\ \Delta\varphi = \frac{\pi}{2N}
\tag{4}
$$

Then the output optical signal of the upper QPSK modulator can be expressed as

$$
\begin{aligned}
E_{up}(t) &= -\frac{\sqrt{2}}{4}E_{in}e^{j\left(\omega_0 t-\frac{\pi}{4}\right)}\sum_{n=-\infty}^{\infty}\cos\left(\frac{\theta_0}{2}-\frac{n\pi}{2}\right)J_n(m_1) \\
&\quad \times \left[\begin{array}{l} e^{j\frac{\pi}{2}}e^{jn\omega t} \\ +e^{jn\left(\omega t+\frac{\pi}{2N}\right)} \end{array}\right]
\end{aligned}
\tag{5}
$$

In the bottom QPSK modulator, the DC bias phases and the phase difference between the two RF signals are identical to the case of the upper QPSK modulator, but the modulation index is
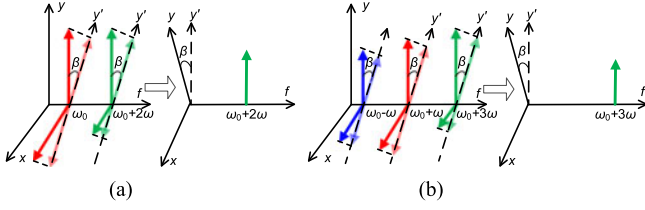
Fig. 3. The principle to generate positive (a) frequency-doubled and (b) frequency-tripled frequency shift signals.

Fig. 4. The simulated results of the generated (a) positive and (b) negative frequency-doubled frequency shift signals.

different. As a result, the bottom QPSK modulator will generate same order optical sidebands but with different powers.

The optical signals output from the two QPSK modulators are combined with orthogonal polarization states through the PBC. Then the orthogonally polarized signal puts into a polarizer (Pol) with its principal axis oriented at an angle of β to one principal axis of the PBC. At the output of the Pol, the optical signal is given by

$$E_{pol}(t) = \frac{1}{\sqrt{2}} \left[E_{up}(t) \cos \beta + E_{bott}(t) \sin \beta \right] \quad (6)$$

According to the analysis above, a frequency-doubled or frequency-tripled optical frequency shifter can be achieved based on high-order SSB modulation and polarization multiplexing, as shown in Fig. 3. Fig. 3(a) shows the principle to generate a positive frequency-doubled frequency shift signal. In the figure, the x and y directions represent the two principal axes of the PBC. At the output of the DP-QPSK modulator, the two second-order SSB modulation signals (optical carriers and upper second-order sidebands) from the two QPSK modulators are polarized along the x and y directions, respectively. Then the Pol is utilized to project the two orthogonally polarized optical signals to one direction (y') for interference. When a proper angle β is set, the optical carriers generated from the two QPSK modulators will have equal power and opposite phase, which makes the optical carriers cancelled each other. Therefore, only the upper second-order sideband is obtained, and a positive frequency-doubled optical frequency shifting is achieved. Fig. 3(b) shows the principle to generate a positive frequency-tripled optical frequency shift signal. The third-order SSB modulation will also generate two first-order sidebands with different powers, but they can be suppressed simultaneously while the upper third-order sideband reserved by the polarization multiplexing and projecting operation.

For the frequency-doubled optical frequency shifter, the parameters can be set as $\theta_0 = 0$, $N = 2$. Then the output optical signal of the Pol can be expressed as

$$E_{pol}(t) = -\frac{1}{4} E_{in} e^{j\omega_0 t} \left[\sqrt{2} J_0(m_1) - 2J_2(m_1) e^{j\frac{\pi}{4}} e^{j2\omega t} \right] \cos \beta$$
$$- \frac{1}{4} E_{in} e^{j\omega_0 t} \left[\sqrt{2} J_0(m_2) - 2J_2(m_2) e^{j\frac{\pi}{4}} e^{j2\omega t} \right] \sin \beta \quad (7)$$

where m_2 is the modulation index of the sub-MZMs in the bottom QPSK modulator. As can be seen, only the optical carriers and upper second-order sidebands are obtained when the higher
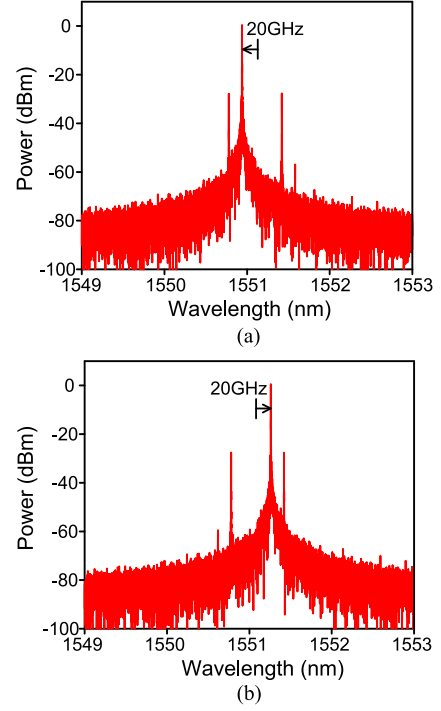
order sidebands are neglected. To suppress the optical carriers, the following condition should be satisfied

$$J_0(m_1) \cos \beta + J_0(m_2) \sin \beta = 0 \quad (8)$$

Considering the complexity of the scheme, the frequency-doubled optical frequency shifter can be further simplified as the bottom QPSK modulator is not modulated by the RF signal but only properly DC biased to suppress the optical carrier terms in equation (7). By adjusting the angle β to make $J_0(m_1)\cos\beta + \sin\beta = 0$, the output of the Pol can be finally expressed as

$$E_{pol}(t) = \frac{1}{2} E_{in} e^{j\frac{\pi}{4}} J_2(m_1) \cos \beta e^{j(\omega_0 + 2\omega)t} \quad (9)$$

As can be seen, the upper second-order sideband is generated while the carriers and other sidebands are suppressed, which obtains a positive frequency shifting of two times the frequency of the RF signal. Similarly, a negative frequency-doubled frequency shifting can be realized by setting $\theta_0 = 0$, $N = -2$.

Fig. 4 shows the simulated results of the frequency-doubled optical frequency shifter. Fig. 4(a) shows the positive frequency shifting while Fig. 4(b) shows the negative frequency shifting. In the simulation, the optical carrier has a wavelength of 1551.1 nm, the frequency of the RF signal is 10 GHz, the modulation index m_1 is 1.50, the angle β is $-25.25°$ and the phase difference $\Delta\varphi$ is set as $45°$ and $-45°$ respectively. As can be seen, an upper or lower second-order sideband is generated, at the same time, higher order sidebands (two fourth-order sidebands with equal power) are also appeared.

For the frequency-tripled optical frequency shifter, the parameters can be set as $\theta_0 = \pi$, $N = 3$. Then the optical signal
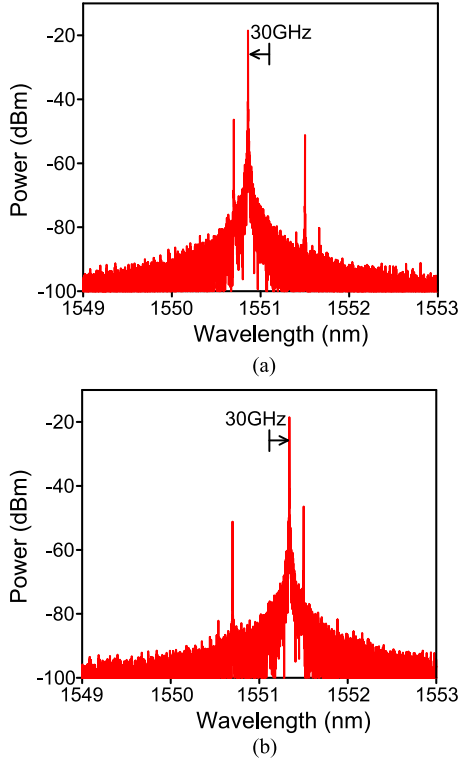
(a)

(b)

Fig. 5. The simulated results of the generated (a) positive and (b) negative frequency-tripled frequency shift signals.

at the output of the Pol is given by

$$E_{pol}(t) = -\frac{1}{4} E_{in} e^{j\frac{\pi}{4}} \begin{bmatrix} J_1(m_1)\left(1 + e^{-j\frac{\pi}{3}}\right) e^{j(\omega_0 - \omega)t} \\ + J_1(m_1)\left(1 + e^{-j\frac{2\pi}{3}}\right) e^{j(\omega_0 + \omega)t} \\ - 2J_3(m_1) e^{j(\omega_0 + 3\omega)t} \end{bmatrix} \cos\beta$$

$$- \frac{1}{4} E_{in} e^{j\frac{\pi}{4}} \begin{bmatrix} J_1(m_2)\left(1 + e^{-j\frac{\pi}{3}}\right) e^{j(\omega_0 - \omega)t} \\ + J_1(m_2)\left(1 + e^{-j\frac{2\pi}{3}}\right) e^{j(\omega_0 + \omega)t} \\ - 2J_3(m_2) e^{j(\omega_0 + 3\omega)t} \end{bmatrix} \sin\beta$$

$$\tag{10}$$

As can be seen, two first-order sidebands and the upper third-order sidebands are obtained when the higher order sidebands are neglected. The two first-order sidebands can be suppressed simultaneously when the following condition is satisfied

$$J_1(m_1)\cos\beta + J_1(m_2)\sin\beta = 0 \tag{11}$$

Then the output optical signal of the Pol can be finally expressed as

$$E_{pol}(t) = \frac{1}{2} E_{in} e^{j\frac{\pi}{4}} \left[J_3(m_1)\cos\beta + J_3(m_2)\sin\beta \right] e^{j(\omega_0 + 3\omega)t} \tag{12}$$

As can be seen, only the upper third-order sideband is reserved, which realizes a positive frequency shifting of three times the frequency of the RF signal. Similarly, a negative frequency shifting with frequency-tripled operation can be realized by setting $\theta_0 = \pi$, $N = -3$.

Fig. 5 shows the simulated results of the frequency-tripled optical frequency shifter. Fig. 5(a) shows the positive frequency
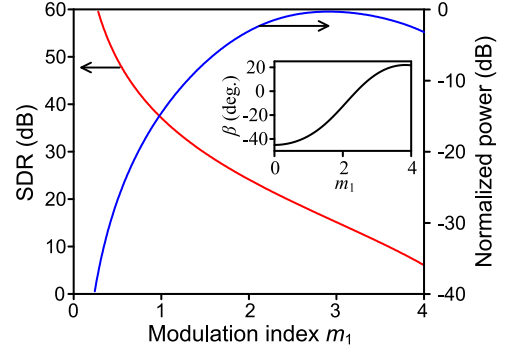

Fig. 6. The calculated SDR and the normalized power of the generated signal varying with the modulation index of the modulator. Inset: the angle β varying with the modulation index.

shifting while Fig. 5(b) shows the negative frequency shifting. In the simulation, the optical carrier has a wavelength of 1551.1 nm, the frequency of the RF signal is 10 GHz, the modulation indices m_1 and m_2 are 1.50 and 1.05 respectively, the angle β is 129.71° and the phase difference $\Delta\varphi$ is set as 30° and $-30°$ respectively. As can be seen, an upper or lower third-order sideband is generated, at the same time, higher order sidebands (two fifth-order sidebands with different power) are also appeared.

The power of the generated frequency shift signal is determined by the signal generated in the two QPSK modulators and the projecting operation in the Pol, as shown in Fig. 3. On the other hand, the higher order sidebands will be also generated, as shown in Figs. 4 and 5. Therefore, the modulation indices of the two QPSK modulators should be optimized to make the generated signal has a high power and a large signal-to-distortion ratio (SDR).

For the frequency-doubled optical frequency shifter, only the modulation index of the upper QPSK modulator needs to be optimized. Assuming that the extinction ratio of the modulator is infinite, then the fourth-order optical sidebands will be the dominate distortion sidebands in the generated signal. The SDR of the generated signal is given by

$$SDR = \left[\frac{2J_2(m_1)}{\left(e^{j\pi/2} + e^{j\pi}\right) J_4(m_1)} \right]^2 \tag{13}$$

Fig. 6 shows the calculated SDR of the generated signal varying with the modulation index of the modulator. As can be seen, the SDR is larger than 20 dB when the modulation index is smaller than 2. The right axis of Fig. 6 shows the power of the generated signal, which normalized by the maximum achievable power and the inset of Fig. 6 shows the angle β varying with the modulation index. As shown in the figure, there is a tradeoff for the modulation index to obtain a frequency-doubled optical frequency shift signal with relatively high power and large SDR simultaneously. In this way, the modulator index of the upper QPSK modulator should be between 1 to 2.

For the frequency-tripled optical frequency shifter, both the modulation indices of the two QPSK modulators need to be optimized. Assuming that the extinction ratio of the modulator is infinite, one of the fifth-order optical sidebands will be the
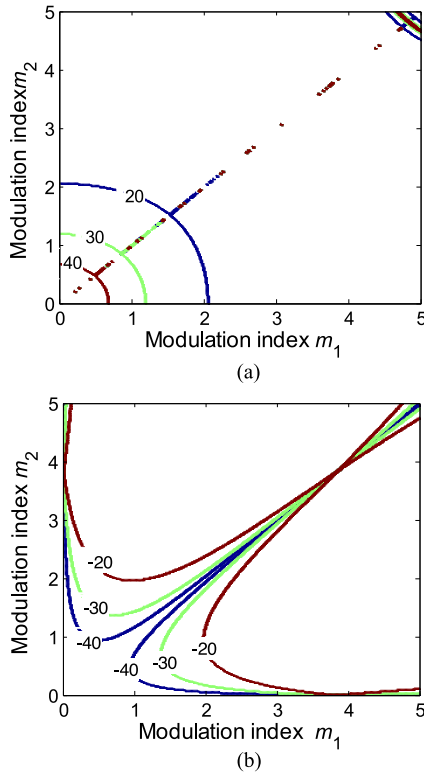
Fig. 7. The contour line of (a) the calculated SDR and (b) the normalized power of the generated signal varying with the two modulation indices.
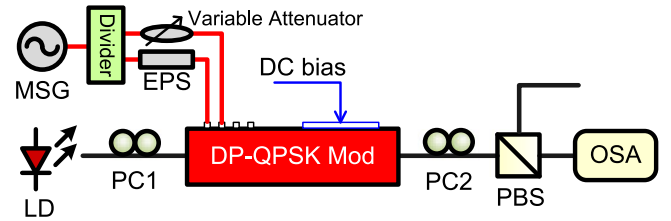

Fig. 8. Experiment setup for frequency-doubled optical frequency shifter (PC: polarization controller; EPS: electrical phase shifter; PBS: polarization beam splitter; OSA: optical spectrum analyzer).

dominate distortion sideband in the generated signal, as shown in Fig. 5. The SDR of the generated signal is given by

$$SDR = \left\{ \frac{J_3\left(m_1\right)\cos\beta - J_3\left(m_2\right)\sin\beta}{\left(1 + e^{j\pi/3}\right)\left[J_5\left(m_1\right)\cos\beta - J_5\left(m_2\right)\sin\beta\right]} \right\}^2 \quad (14)$$

Fig. 7(a) shows the contour line of the calculated SDR for the generated signal varying with the two modulation indices. As can be seen, the SDR can be larger than 20 dB when both the modulation indices are smaller than 2. Fig. 7(b) shows the contour line of the calculated power for the generated signal, which normalized by the maximum achievable power. As shown in the figures, to obtain a frequency-tripled optical frequency shift signal with relatively high power and large SDR simultaneously, the modulator indices of the two QPSK modulators should be set properly.

To adjust the frequency shifting of the generated optical signal, only the frequency of the RF signal should be changed, and the generated optical frequency shifting is two or three times the frequency of the RF signal. Therefore, the frequency tuning operation of the proposed scheme is simple, flexible and accurate. The maximum frequency shifting range is three times the maximum frequency of the drive signal source and the bandwidth of the modulator, which can reach 40 GHz in laboratory environment. As a result, a frequency shifting from more than negative 100 GHz to more than positive 100 GHz can possibly be generated with the proposed scheme.

III. EXPERIMENT SETUP AND RESULTS

An experiment for the generation of a frequency-doubled optical frequency shift signal is carried out as shown in Fig. 8. In the experiment, a CW light is generated from an LD (Agilent N7714A) with a wavelength of 1551.1 nm and a power of 13 dBm. The light is adjusted by a polarization controller (PC1) and then sent to a DP-QPSK modulator (Fujitsu FTM7977HQA) which has a half-wave voltage of about 3.5 V and an optical insertion loss of 13 dB. An RF signal is provided by a microwave signal generator (MSG) (Agilent E8257D) with a frequency of 5 GHz and a power of 23.7 dBm. The RF signal is split to two parts through an electrical power divider, and then sent to two RF ports of the upper QPSK modulator. In one path of the RF signals an electrical phase shifter (EPS) is inserted to introduce a phase difference of 45° or −45°, while in another path, a variable attenuator is employed to compensate the power imbalance of the two RF signals caused by the insertion loss of the EPS. Another PC (PC2) combined with a polarization beam splitter (PBS) works as a Pol to obtain frequency shift signals. The optical signals are measured by an optical spectrum analyzer (OSA) (Yokogawa AQ6370C) with a resolution of 0.02 nm.

Fig. 9(a) shows the spectrum of the generated positive frequency shift signal. As can be seen, the generated sideband and the optical carrier have a frequency space of 10 GHz, which two times of the frequency of the RF signal. Due to the finite extinction ratio of the modulator, the carrier and the lower second-order sideband are not totally suppressed, and the first-order sidebands are also generated, but the upper second-order sideband is 27 dB higher than the other frequency components. Fig. 9(b) shows the spectrum of the generated negative frequency shift signal, the frequency of the generated sideband is 10 GHz smaller than the optical carrier, and the SDR of the generated signal is 25 dB, as shown in the figure. The SDR is larger than the results reported in [13], [14] and [16], and it can satisfy the requirement of most applications [13], [15], [19], [20].

The optical loss of the frequency shifter is also investigated. The loss has three origins. The first kind is the insertion loss of the optical components, including 13 dB loss of the modulator and 7 dB loss of the two PCs and the PBS. The second kind is the modulation loss in the modulator, which including the normalized power loss of about 7 dB (modulation index at 1.5, as shown in Fig. 6) and the minimum achievable power loss of 9 dB (maximum value of $1/2J_2^2(m)$). The third kind is the polarization project operation in the PBS, which is about 11 dB
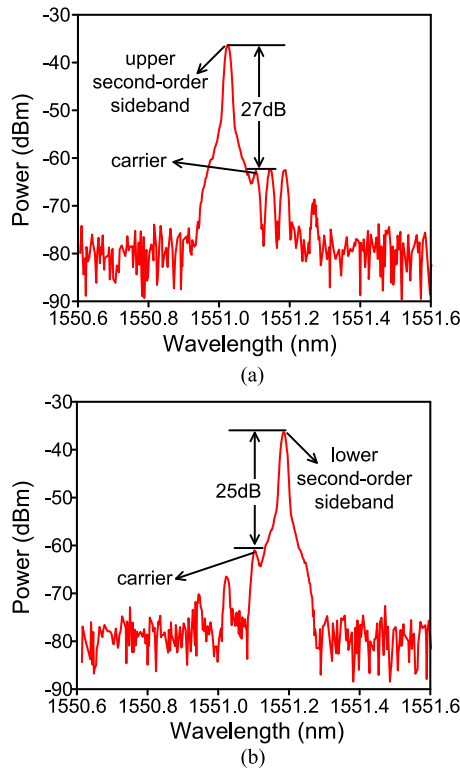
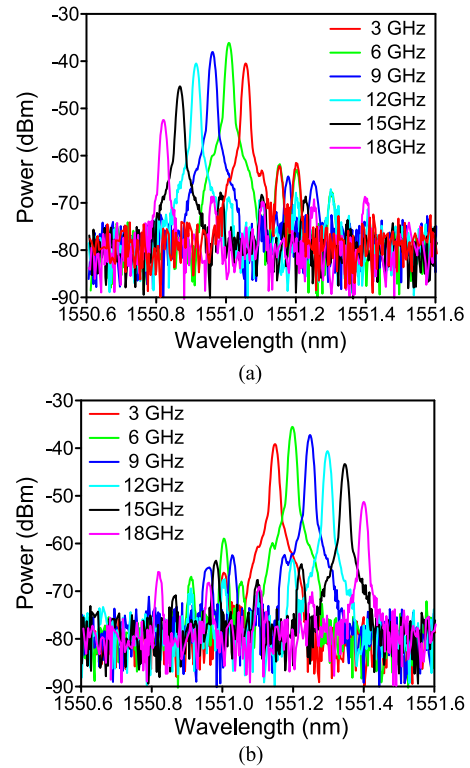Fig. 9. The spectra of (a) the positive and (b) the negative frequency-doubled frequency shift signals.

Fig. 10. The spectra of (a) the positive and (b) the negative frequency-doubled frequency shift signals with different input RF frequencies.

(value of $1/2\cos^2\beta$). The modulation loss is in the same range reported in [5] and [15] (16 dB and 17 dB, respectively). The insertion loss is similar to the result in [15] (19 dB, including 6 dB of the modulator and 13 dB of the optical filter) but larger compared to the result in [5] (7 dB of the QPSK modulator), however, it can be decreased by selecting components with small insertion losses. On the other hand, the increment of the projection loss is the cost of achieving high-order optical frequency shifting, and it can be compensated by using an optical amplifier followed by the PBS.

To verify the frequency tunability of the proposed scheme, the frequency of the RF signal is tuned from 3 GHz to 18 GHz while the other parameters keep unchanged. Figs. 10(a) and (b) show the spectra of the generated positive and negative frequency-doubled frequency shift signals, respectively. As shown in the figure, one single sideband with a frequency space of two times the frequency of the RF signal is obtained while the other sidebands are effectively suppressed. The frequency shifting of the generated signal can be simply tuned by adjusting the frequency of the RF signal, the scheme has good tunability. It can also be seen that, the power of the generated signals are different, this is caused by the operation bandwidth of the variable attenuator (DC-12 GHz) and the electrical divider (2–18 GHz).

Due to the finite extinction ratio of the modulator, carrier and other sidebands will also be generated and the SDR of the frequency shift signal will be deteriorated. Fig. 11 shows the experimental results of the SDR varying with the frequency shifting of the generated signals. As can be seen, the SDR changed randomly, but a SDR higher than 20 dB can be obtained when
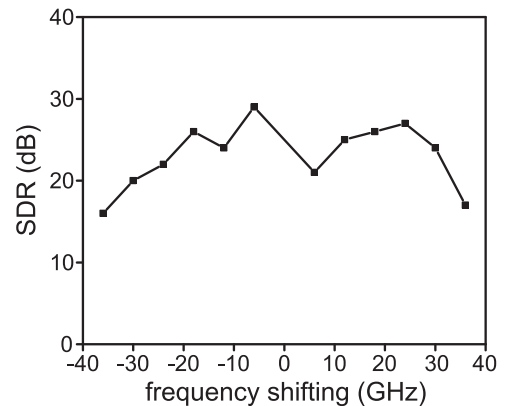

Fig. 11. The experimental results of the SDR varying with the frequency shifting.

the frequency shifting is smaller than 30 GHz. The SDRs of the signals with frequency shifting of 36 GHz are relatively small, this is because the cutoff frequencies of the variable attenuator and the electrical divider inducing a power decrement of the second-order optical sideband. When electrical components with broader bandwidths are used, a larger frequency shifting with a higher SDR can be achieved.

In the experiment, the long-term stability of the proposed scheme is relatively poor, due to the drifting of the DC bias points in the integrated modulator. This problem can be resolved by employing a DP-QPSK modulator Bias Controller (i.e. YY LABS Inc. D0158) in the system.

IV. Conclusion

We propose and experimentally demonstrate a novel scheme to generate frequency-doubled or frequency-tripled optical frequency shifter using an integrated DP-QPSK modulator based on high order SSB modulation and polarization multiplexing. By changing the DC bias phases of the modulator and the phase difference between the input RF signals, positive or negative frequency shifting with frequency multiplication can be achieved. The scheme is numerically analyzed with the modulation indices of the modulator for optimal operation. The SDR performance is theoretically analyzed and experimentally investigated. Experiment results show that the scheme has good tunability, it can generate a continuous frequency shifting ranged from -30 to 30 GHz with a SDR higher than 20 dB. The frequency tuning operation is simple, accurate and flexible.

References

[1] K. Wang and L. Zeng. "Double-grating frequency shifter for low-coherence heterodyne interferometry," *Opt. Commun.*, vol. 251, pp. 1–5, Jul. 2005.

[2] A. Kanno *et al.*, "16-Gbaud QPSK radio transmission using optical frequency comb with recirculation frequency shifter for 300-GHz RoF signal," in *Proc. IEEE Int. Top. Meeting Microw. Photon.*, 2012, vol. 83, no. 1, pp. 298–301.

[3] A. Dorrington and R. Kunnemeyer, "Single sideband techniques for laser Doppler velocimeter frequency offset," *Opt. Eng.*, vol. 42, no. 11, pp. 3239–3246, Nov. 2003.

[4] C. Dorrer and I. Kang, "Highly sensitive direct characterization of femtosecond pulses by electro-optic spectral shearing interferometry," *Opt. Lett.*, vol. 28, no. 6, pp. 477–479, Mar. 2003.

[5] J. Zhang *et al.*, "Stable optical frequency-locked multicarriers generation by double recirculating frequency shifter loops for Tb/s communication," *J. Lightw. Technol.*, vol. 30, no. 24, pp. 3938–3945, Dec. 2012.

[6] Z. Wang, T. Yang, D. Jia, Z. Wang, and M. Sang, "An FBG sensor interrogation technique based on a precise optical recirculating frequency shifter driven by RF signals," *Proc. SPIE*, vol. 8624, pp. 1–12, Feb. 2013, Art no. 8624w.

[7] H. Yamazaki *et al.*, "Dual-carrier dual-polarization IQ modulator using a complementary frequency shifter," *IEEE J. Sel. Topics Quantum Electron.*, vol. 19, no. 6, pp. 175–182, Nov./Dec. 2013.

[8] B. Gouhier, K. Lee, A. Nirmalathas, C. Lim and E. Skafidas, "A flexible, wide bandwidth electro-optic probing system using a recirculating frequency shifter," in *Proc. Int. Topical Meeting Microw. Photon./2014 9th Asia-Pacific Microw. Photon. Conf.*, 2014, pp. 327–330.

[9] K. Nosu, S. Rashleigh, H. Taylor, and J. Weller. "Acousto-optic frequency shifter for single-mode fibres," *Electron. Lett.*, vol. 19, no. 20, pp. 816–818, Sep. 1983.

[10] E. Barretto and J. Hvam, "Photonic integrated single-sideband modulator/frequency shifter based on surface acoustic waves," *Proc. SPIE*, vol. 7719, pp. 1–12, Apr. 2010, Art. no. 771920.

[11] Y. Li, S. Meersman and R. Baets, "Optical frequency shifter on SOI using thermo-optic serrodyne modulation," in *Proc. 7th IEEE Int. Conf. Group IV Photon.*, 2010, pp. 75–77.

[12] K. Shibuya, S. Hisatake, and T. Kobayashi, "10-GHz-order high-efficiency electrooptic frequency shifter using slant-periodic domain inversion," *IEEE Photon. Techn. Lett.*, vol. 16, no. 8, pp. 1939–1941, Aug. 2004.

[13] M. Frankel and R. Esman, "optical single-sideband suppressed-carrier modulator for wide-band signal processing," *J. Lightw. Technol.*, vol. 16, no. 5, pp. 859–863, May 1998.

[14] A. Loayssa, D. Benito, and M. J. Garde, "Single-sideband suppressed-carrier modulation using a single-electrode electrooptic modulator," *IEEE Photon. Technol. Lett.*, vol. 13, no. 8, pp. 869–871, Aug. 2001.

[15] S. Xiao, and A. Weiner, "Optical carrier-suppressed single sideband (O-CS-SSB) modulation using a hyperfine blocking filter based on a virtually imaged phased-array (VIPA)," *IEEE Photon. Technol. Lett.*, vol. 17, no. 7, pp. 1522–1524, Jul. 2005.

[16] A. Campillo, "Polarization-based single-sideband suppressed carrier modulator," *IEEE Photon. Technol. Lett.*, vol. 18, no. 16, pp. 1780–1782, Aug. 2006.

[17] J. Zhang *et al.*, "Theoretical and experimental study on improved frequency-locked multicarrier generation by using recirculating loop based on multifrequency shifting single-sideband modulation," *IEEE Photon. J.*, vol. 4, no. 6, pp. 2249–2261, Dec. 2012.

[18] S. Hisatake, T. Konishi, and T. Nagatsuma, "Multiplication operation of an optical frequency shifter using cascaded electrooptic traveling phase grating," in *Proc. Eur. Conf. Lasers Electro-Opt. Eur. Quantum Electron. Conf.*, 2009, vol. 26, no. 9, pp. 1–1.

[19] A. Loayssa, C. Lim, A. Nirmalathas, and D. Benito, "Optical single-sideband modulator for broad-band subcarrier multiplexing system," *IEEE Photon. Technol. Lett.*, vol. 15, no. 2, pp. 311–313, Feb. 2003.

[20] J. Palací and B. Vidal, "Tunable optical delay line based on single-sideband suppressed-carrier modulation," *IEEE Photon. Technol. Lett.*, vol. 25, no. 1, pp. 43–46, Jan. 2013.

Xuan Li received the B.E. and M.E. degrees in 2011 and 2014, respectively, from the School of Information and Navigation, Air Force Engineering University, Xi'an, China, where he is currently working toward the Ph.D. degree. From March 2015 to June 2016, he was with the Microwave Photonics Research Laboratory, College of Electronic and Information Engineering, Nanjing University of Aeronautics and Astronautics, Nanjing, China. His current research interests include arbitrary waveform generation and signal processing.

Shanghong Zhao received the B.S. and M.S. degrees from the Physics Department, Lanzhou University, Lanzhou, China, in 1984 and 1989, respectively, and the Ph.D. degree from Xi'an Institute of Optics and Precision Mechanics of CAS in 1998. He is currently a Full Professor in the School of Information and Navigation, Air Force Engineering University, Xi'an, China. His research interests include laser technology, optical satellite communication, and networking.

Zihang Zhu received the B.E., M.E., and Ph.D. degrees from the Air-to-Ground Communication Department, Telecommunication Engineering College, Air Force Engineering University, Xi'an, China, in 2007, 2009, and 2015, respectively. He is currently a Lecturer in the School of Information and Navigation, Air Force Engineering University. His research interests include photonic generation of microwave signals, intersatellite microwave photonics links, and radio-over-fiber systems.

Kun Qu received the B.E. degree from the School of Information and Navigation, Air Force Engineering University, Xi'an, China, in 2012 and the M.E. degree from the Science College, Air Force Engineering University in 2015. He is currently working toward the Ph.D. degree in the School of Information and Navigation, Air Force Engineering University. His current research interests include optical frequency-comb generation and photonic analogy-to-digital conversion.

Tao Lin received the B.E. degree from the School of Information and Navigation, Air Force Engineering University, Xi'an, China, in 2015, where he is currently working toward the M.E. degree. His current research interests include optical frequency-comb generation and photonic microwave frequency conversion.

Shilong Pan received the B.S. and Ph.D. degrees in electronics engineering from Tsinghua University, Beijing, China, in 2004 and 2008, respectively. From 2008 to 2010, he was a Vision 2010 Postdoctoral Research Fellow in the Microwave Photonics Research Laboratory, University of Ottawa, Ottawa, ON, Canada. He is currently a Full Professor and the Executive Director of the Key Laboratory of Radar Imaging and Microwave Photonics, Nanjing University of Aeronautics and Astronautics, Ministry of Education, Nanjing, China.